A Fast and Reliable Pick-and-Place Application with a Spherical Soft Robotic Arm

Online appendix

Author(s):
Zughaibi, Jasan; Hofer, Matthias; D'Andrea, Raffaello

Publication date:
2021

Permanent link:
https://doi.org/10.3929/ethz-b-000470203

Online Appendix - A Fast and Reliable Pick-and-Place Application with a Spherical Soft Robotic Arm

Jasan Zughaibi, Matthias Hofer, and Raffaello D'Andrea

I. Introduction

In this online appendix we present the Delta Representation in more detail. In particular, we provide a detailed mathematical analysis, discuss its properties and show further validation experiments.

II. Control Allocation

In this section, the mathematical details of the control allocation mapping are discussed.

A. Pressure Difference

In the case of two actuators, it is straightforward to define the pressure difference. In the case of three actuators A, B, and C, we define the pressure difference as the difference between two subsequent actuators, namely,

$$\Delta p_{AB} \coloneqq p_A - p_B, \qquad \Delta p_{BC} \coloneqq p_B - p_C. \tag{1}$$

The definition is arbitrary as long as each pressure occurs at least once in the equations. The difficulty lies in the determination of the inverse, i.e. the relation from $\Delta p_{AB}, \Delta p_{BC}$ to p_A, p_B, p_C. Only two equations are provided in (1), which contain three unknowns. In order to obtain a unique solution for the inverse problem, a third variable $\bar{p}$ is required. Consider the constrained linear system of equations

$$\begin{bmatrix} 1 & -1 & 0 \\ 0 & 1 & -1 \end{bmatrix} \begin{bmatrix} p_A \\ p_B \\ p_C \end{bmatrix} = \begin{bmatrix} \Delta p_{AB} \\ \Delta p_{BC} \end{bmatrix} \tag{2}$$

subject to

$$p_A \geq \bar{p}, \tag{3}$$
$$p_B \geq \bar{p}, \tag{4}$$
$$p_C \geq \bar{p}, \tag{5}$$
$$\min\{p_A, p_B, p_C\} = \bar{p}. \tag{6}$$

The unique solution of (2)-(6) is given by

$$p_A = \max\{\bar{p}, \bar{p} + \Delta p_{AB}, \bar{p} + \Delta p_{AB} + \Delta p_{BC}\} \tag{7}$$
$$p_B = \max\{\bar{p}, \bar{p} + \Delta p_{BC}, \bar{p} - \Delta p_{AB}\} \tag{8}$$
$$p_C = \max\{\bar{p}, \bar{p} - \Delta p_{BC}, \bar{p} - \Delta p_{AB} - \Delta p_{BC}\}. \tag{9}$$

Proof: First, we show that Equations (7)-(9) satisfy the linear system of equations in (2). Equations (7)-(9) can be rewritten as

$$p_A = \begin{cases} \bar{p} & , \Delta p_{AB}, \Delta p_{BC} \in S_{++} \\ \bar{p} + \Delta p_{AB} & , \Delta p_{AB}, \Delta p_{BC} \in S_{-+} \\ \bar{p} + \Delta p_{AB} + \Delta p_{BC} & , \Delta p_{AB}, \Delta p_{BC} \in S_{--} \end{cases} \tag{10}$$

$$p_B = \begin{cases} \bar{p} - \Delta p_{AB} & , \Delta p_{AB}, \Delta p_{BC} \in S_{++} \\ \bar{p} & , \Delta p_{AB}, \Delta p_{BC} \in S_{-+} \\ \bar{p} + \Delta p_{BC} & , \Delta p_{AB}, \Delta p_{BC} \in S_{--} \end{cases} \tag{11}$$

$$p_C = \begin{cases} \bar{p} - \Delta p_{AB} - \Delta p_{BC} & , \Delta p_{AB}, \Delta p_{BC} \in S_{++} \\ \bar{p} - \Delta p_{BC} & , \Delta p_{AB}, \Delta p_{BC} \in S_{-+} \\ \bar{p} & , \Delta p_{AB}, \Delta p_{BC} \in S_{--} \end{cases}, \tag{12}$$

The authors are members of the Institute for Dynamic Systems and Control, ETH Zurich, Switzerland. {zjasan, hofermat, rdandrea}@ethz.ch

where

$$S_{++} = \big\{(\Delta p_{AB}, \Delta p_{BC}) \in \mathbb{R}^2 \big| \Delta p_{AB} \leq 0,\, \Delta p_{AB} + \Delta p_{BC} \leq 0\big\} \tag{13}$$

$$S_{-+} = \big\{(\Delta p_{AB}, \Delta p_{BC}) \in \mathbb{R}^2 \big| -\Delta p_{AB} \leq 0,\, \Delta p_{BC} \leq 0\big\} \tag{14}$$

$$S_{--} = \big\{(\Delta p_{AB}, \Delta p_{BC}) \in \mathbb{R}^2 \big| -\Delta p_{BC} \leq 0,\, -\Delta p_{AB} - \Delta p_{BC} \leq 0\big\}. \tag{15}$$

Equations (10)-(12) allow us to compute the differences $p_A - p_B$ and $p_B - p_C$ in a more intuitive way. Clearly, $p_A - p_B = \Delta p_{AB}$ and $p_B - p_C = \Delta p_{BC}$. Hence, the linear system of equations in (2) is satisfied by (7)-(9).
It remains to show that the constraints (3)-(6) are satisfied. From (10)-(12) and from the definitions of the corresponding domains in (13)-(15), it is clear that the inequality constraints in (3)-(5) are satisfied. The equality constraint (6) implies that at least one of the inequality constraints must always be active. Note that

$$S_{++} \cup S_{-+} \cup S_{--} = \mathbb{R}^2, \tag{16}$$

$$\big(S_i \backslash \partial S_i\big) \cap \big(S_j \backslash \partial S_j\big) = \emptyset,\, i \neq j \tag{17}$$

Hence, a given pair $\Delta p_{AB}, \Delta p_{BC}$ is an element in the interior of either S_{++}, S_{-+}, or S_{--} or lies on the boundaries ∂S_i. Accordingly, from (10)-(12) it is clear that for a given pair $\Delta p_{AB}, \Delta p_{BC}$, at least one of the pressures p_i is restricted to $\bar{p}$. This concludes the proof. ■

Working in terms of pressure differences entails a desirable invariance property. Assume $\Delta p_{AB}(t), \Delta p_{BC}(t)$ are periodic, bounded, and piecewise continuous functions with the property

$$\int_0^{\delta_1} \Delta p_{AB}(t)\mathrm{d}t = 0, \qquad \int_0^{\delta_2} \Delta p_{BC}(t)\mathrm{d}t = 0, \tag{18}$$

where δ_1, δ_2 are the periods such that $\Delta p_i(t) = \Delta p_i(t + \delta_i)\, \forall t \in \mathbb{R}$. Let δ be the least common multiple of δ_1 and δ_2. Then:

$$\int_0^{\delta} p_A(t)\mathrm{d}t = \int_0^{\delta} p_B(t)\mathrm{d}t = \int_0^{\delta} p_C(t)\mathrm{d}t\,, \tag{19}$$

when p_A, p_B, and p_C are related to Δp_{AB}, Δp_{BC} as specified in (1).

Proof: As δ represents the least common multiple of the periods δ_1 and δ_2, the equations in (18) can be written as

$$\int_0^{\delta} \Delta p_{AB}(t)\mathrm{d}t = 0, \qquad \int_0^{\delta} \Delta p_{BC}(t)\mathrm{d}t = 0. \tag{20}$$

Substituting the definitions in (1) and considering the linearity of the integral operator, results in

$$\int_0^{\delta} \big(p_A(t) - p_B(t)\big)\mathrm{d}t = 0 \tag{21}$$

$$\Leftrightarrow \int_0^{\delta} p_A(t)\mathrm{d}t = \int_0^{\delta} p_B(t)\mathrm{d}t \tag{22}$$

and similarly for Δp_{BC}. This concludes the proof. ■

The reader is referred to Section III, where the system is excited with signals satisfying the property in (18), as part of the experimental validation.

B. Decoupling

The mapping introduced in the previous paragraph allows us to represent a pressure point (p_A, p_B, p_C) in terms of two pressure differences $\Delta p_{AB}, \Delta p_{BC}$ and a lower pressure bound $\bar{p}$. While the pressure differences are directly coupled to the angular deflection, the lower pressure bound $\bar{p}$ is related to the stiffness of the system. In general, the pressure differences $\Delta p_{AB}, \Delta p_{BC}$ are scalar quantities. However, associated directions of action can be assigned when introducing a kinematic model of the robot arm. These associated directions of action depend on the actuator configuration and the definition of the pressure differences. By explicitly computing the associated directions of action, a transformation can be introduced which aligns the pressure differences $\Delta p_{AB}, \Delta p_{BC}$ with the orientations α, β of the robot arm. Note that in principle any nonlinear model is suitable for computing the associated directions of action. However, for the sake of simplicity, we restrict the discussion to a linear model. A simple kinematic model, relating the pressures p_A, p_B, and p_C to the orientation α, β is introduced in the previous work [1], namely,

$$\begin{bmatrix}\alpha \\ \beta\end{bmatrix} \propto \begin{bmatrix} 0 & \cos(\pi/6) & -\cos(\pi/6) \\ -1 & \sin(\pi/6) & \sin(\pi/6) \end{bmatrix} \begin{bmatrix} p_A \\ p_B \\ p_C \end{bmatrix}. \tag{23}$$

We rewrite (23) in terms of pressure differences by incorporating the definitions in (1). Clearly, $\alpha \propto \sqrt{3}/2\Delta p_{BC}$. It follows for β that,

$$\beta \propto -p_A + \frac{1}{2}p_B + \frac{1}{2}p_C + \underbrace{\frac{1}{2}p_B - \frac{1}{2}p_B}_{=0} \tag{24}$$

$$\propto -(p_A - p_B) - \frac{1}{2}(p_B - p_C) \tag{25}$$

$$\propto -\Delta p_{AB} - \frac{1}{2}\Delta p_{BC}\,. \tag{26}$$

Accordingly, we define the decoupled pressure differences as

$$\begin{bmatrix}\Delta p_\alpha \\ \Delta p_\beta\end{bmatrix} \coloneqq \underbrace{\begin{bmatrix}0 & \sqrt{3}/2 \\ -1 & -1/2\end{bmatrix}}_{T} \begin{bmatrix}\Delta p_{AB} \\ \Delta p_{BC}\end{bmatrix} \tag{27}$$

which are aligned with the orientations α and β. The linear transformation T is invertible. The inverse is given by

$$T^{-1} = \begin{bmatrix}-1/\sqrt{3} & -1 \\ 2/\sqrt{3} & 0\end{bmatrix}. \tag{28}$$

C. Composition

The composition of the mappings introduced in the two previous sections allows us to define a bijective mapping ξ. We refer to the mapping as the Delta Representation. The Delta Representation can be considered as a control allocation which significantly simplifies the modeling and control due to its decoupling characteristics. A change with respect to Δp_α solely affects the orientation α and analogously for Δp_β and β,

$$\Delta p_\alpha \to \alpha, \qquad \Delta p_\beta \to \beta. \tag{29}$$

Given the two virtual control inputs $\Delta p_\alpha, \Delta p_\beta$, and the lower pressure bound $\bar{p}$, the absolute pressures p_A, p_B, and p_C can be computed as

$$\xi : \begin{bmatrix}\Delta p_\alpha \\ \Delta p_\beta \\ \bar{p}\end{bmatrix} \longmapsto \begin{bmatrix}p_A \\ p_B \\ p_C\end{bmatrix} \tag{30}$$

with

$$\begin{aligned} p_A &= \max\{\bar{p}, \bar{p} + \Delta p_{AB}, \bar{p} + \Delta p_{AB} + \Delta p_{BC}\} \\ p_B &= \max\{\bar{p}, \bar{p} + \Delta p_{BC}, \bar{p} - \Delta p_{AB}\} \\ p_C &= \max\{\bar{p}, \bar{p} - \Delta p_{BC}, \bar{p} - \Delta p_{AB} - \Delta p_{BC}\} \end{aligned} \qquad \text{where} \qquad \begin{bmatrix}\Delta p_{AB} \\ \Delta p_{BC}\end{bmatrix} = T^{-1}\begin{bmatrix}\Delta p_\alpha \\ \Delta p_\beta\end{bmatrix}.$$

For instance, the mapping ξ is used to relate the controller outputs Δp_α, Δp_β to the physical control inputs p_A, p_B, p_C and is straightforward to implement. The inverse function ξ^{-1} is given by

$$\xi^{-1} : \begin{bmatrix}p_A \\ p_B \\ p_C\end{bmatrix} \longmapsto \begin{bmatrix}\Delta p_\alpha \\ \Delta p_\beta \\ \bar{p}\end{bmatrix} \tag{31}$$

with

$$\begin{aligned} \begin{bmatrix}\Delta p_\alpha \\ \Delta p_\beta\end{bmatrix} &= T\begin{bmatrix}\Delta p_{AB} \\ \Delta p_{BC}\end{bmatrix} \\ \bar{p} &= \min\{p_A, p_B, p_C\}\,. \end{aligned} \qquad \text{where} \qquad \begin{aligned} \Delta p_{AB} &= p_A - p_B \\ \Delta p_{BC} &= p_B - p_C. \end{aligned}$$

III. Experimental Validation

In this section, we experimentally validate the decoupling characteristics of the Delta Representation. First, we investigate the effect of a change with respect to Δp_α on the orientation of the robot arm for different levels of $\bar{p}$, while keeping Δp_β constant. Subsequently, we investigate the effect of a simultaneous excitation in Δp_α and Δp_β. The trajectories in $\Delta p_\alpha, \Delta p_\beta$, and $\bar{p}$ are transferred offline to pressure setpoint trajectories $p_{A,SP}, p_{B,SP}$, and $p_{C,SP}$ using Equation (30). The pressure setpoint trajectories are tracked using three independent Proportional-Integral-Derivative pressure controllers. Notice that there is no angle control applied.

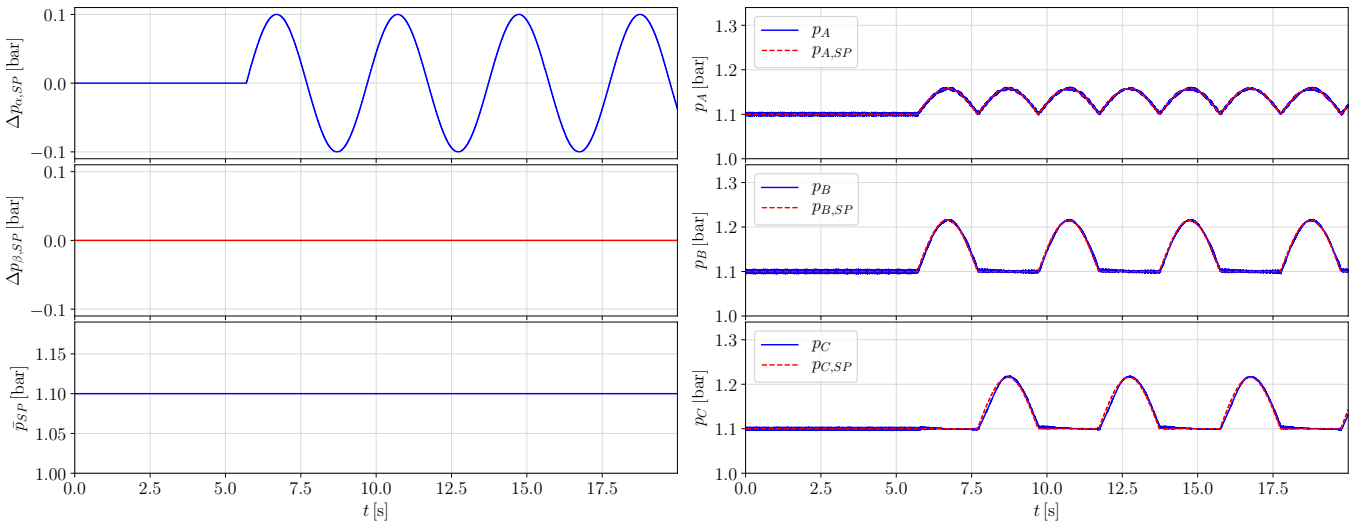

Fig. 1. The figure shows the relation between pressure setpoint trajectories in the Delta Representation space (left) and the corresponding trajectories in the absolute pressure space (right), computed using Equation (30). The pressure setpoints $p_{i,SP}$, $i = A, B, C$ are tracked using three independent Proportional-Integral-Derivative controllers. Notice that at least one of the pressures p_i, $i = A, B, C$ is always restricted to $\bar{p}$.

A. Variation in Δp_α

We apply a sinusoidal trajectory with a fixed amplitude and frequency in Δp_α. The objective is to investigate the effect on the orientation of the robot arm for three different levels of $\bar{p}$. Fig. 1 shows the pressure setpoint trajectories in the Delta Representation space and the resulting trajectories in the absolute pressure space, for $\bar{p} = 1.10\,\text{bar}$. Fig. 2 shows the resulting angular trajectories for three different levels of $\bar{p}$. As expected, a sinusoid with respect to Δp_α causes a sinusoid in α, while β remains almost constant, as $\Delta p_{\beta,SP} = 0$. For increasing levels of $\bar{p}$ the resulting amplitude in α decreases.

B. Simultaneous Variation in Δp_α and Δp_β

We apply sinusoidal trajectories with respect to Δp_α and Δp_β with a phase shift of $\pi/2$ for a fixed value of $\bar{p}$. Fig. 3 shows the pressure setpoint trajectories in the Delta Representation space and the corresponding trajectories in the absolute pressure space. Notice that the applied signals satisfy the property in (18). Accordingly, the invariance property with respect to the integral in (19) is satisfied, as can be seen in Fig. 3 (right). The resulting effect on the orientation of the robot arm is depicted in Fig. 4, illustrating the decoupling characteristics of the control allocation proposed.

C. Discussion

The Delta Representation induces a similarity property between the angle and pressure space. Instead of directly controlling the absolute pressures p_A, p_B, p_C, we introduce an intermediate control input state $\Delta p_\alpha, \Delta p_\beta, \bar{p}$ by

1. considering pressure differences $\Delta p_{AB} = p_A - p_B$ and $\Delta p_{BC} = p_B - p_C$ between the actuators,
2. transforming the associated directions of action such that the pressure differences are aligned with the orientation of the robot arm.

Note that both components of the mapping are necessary to induce the similarity property. The first component maps the absolute pressure space, which is restricted to positive values, onto a domain that is centered around zero by considering the pressure difference between the actuators. A change with respect to the pressure differences causes a change in the angular deflection of the robot arm in certain directions. The second component of the mapping aligns these directions with the orientations of the robot arm, allowing us to consider the system as decoupled. Note that there is no angle control applied in the validation experiments. Accordingly, small deviations in the decoupling can be observed, which are mainly caused by imperfections in the actuator mounting, the small angle assumption of the kinematic model, boundary effects, and viscoelastic material behavior.

While the virtual control inputs Δp_α, Δp_β affect the orientation of the robot arm, the parameter $\bar{p}$ is related to the stiffness of the system. An important characteristic of the Delta Representation is that it preserves the stiffness of the system. More specifically, the parameter $\bar{p}$ is not influenced in a motion control system. At all times, at least one of the actuator pressures is restricted to $\bar{p}$. Accordingly, the Delta Representation addresses the issue discussed in [2], namely that feedback control in general imposes a reduction in compliance to increase the tracking performance in soft robotic systems. However, by leveraging the Delta Representation, $\bar{p}$ remains an independent degree of freedom and can be specified by the user.

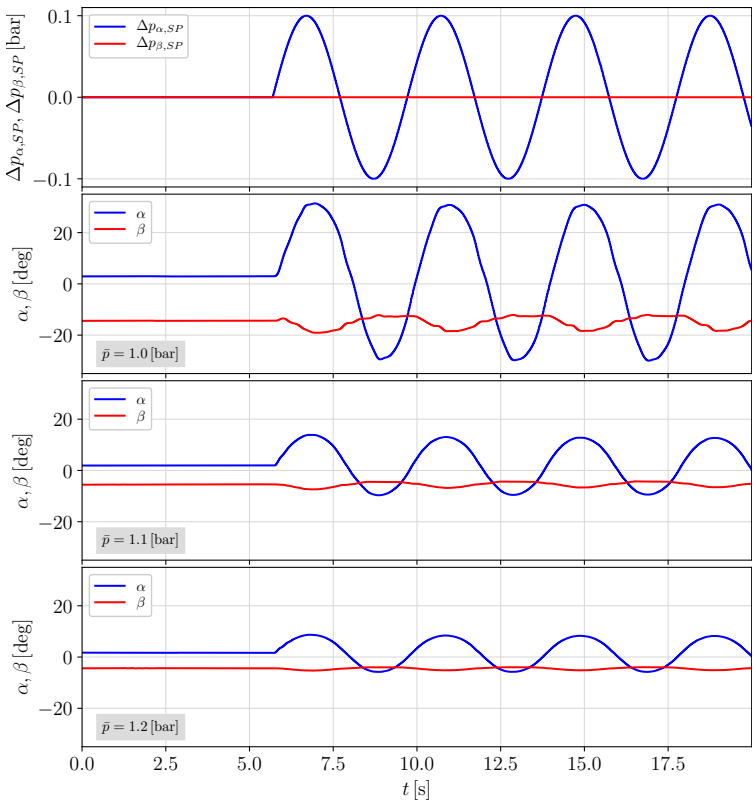

Fig. 2. The figure shows the results of a verification experiment of the decoupling characteristics of the Delta Representation. A sinusoid with respect to Δp_α is applied (top plot) and the effect on the orientation of the robot arm is shown for three different levels of $\bar{p}$ (three bottom plots). While β remains constant (in approximation) due to $\Delta p_{\beta,SP} = 0$, sinusoidal trajectories with respect to α can be observed, illustrating the decoupling characteristics of the control allocation mapping. The constant offsets are caused by viscoelastic material behavior.

IV. Alternative Formulation

Alternatively to the constrained linear system of equations (2)-(6), the inverse function of the pressure difference mapping can be derived from the following optimization problem.

$$\min_{p_A, p_B, p_C} \frac{1}{2}(\Delta p_{AB} - (p_A - p_B))^2 + \frac{1}{2}(\Delta p_{BC} - (p_B - p_C))^2 \tag{32}$$

subject to

$$p_A \geq \bar{p} \tag{33}$$

$$p_B \geq \bar{p} \tag{34}$$

$$p_C \geq \bar{p} \tag{35}$$

$$\min\{p_A, p_B, p_C\} = \bar{p} \tag{36}$$

Solving (32)-(36) analytically results in (7)-(9). Accordingly, the optimization problem is solved at zero cost. The formulation of the problem as an optimization problem might be interesting for numerical implementations.

References

[1] M. Hofer and R. D'Andrea, "Design, fabrication, modeling and control of a fabric-based spherical robotic arm," *Mechatronics*, vol. 68, 2020.

[2] C. Della Santina, M. Bianchi, G. Grioli, F. Angelini, M. Catalano, M. Garabini, and A. Bicchi, "Controlling soft robots: Balancing feedback and feedforward elements," *IEEE Robotics Automation Magazine*, vol. 24, no. 3, 2017.

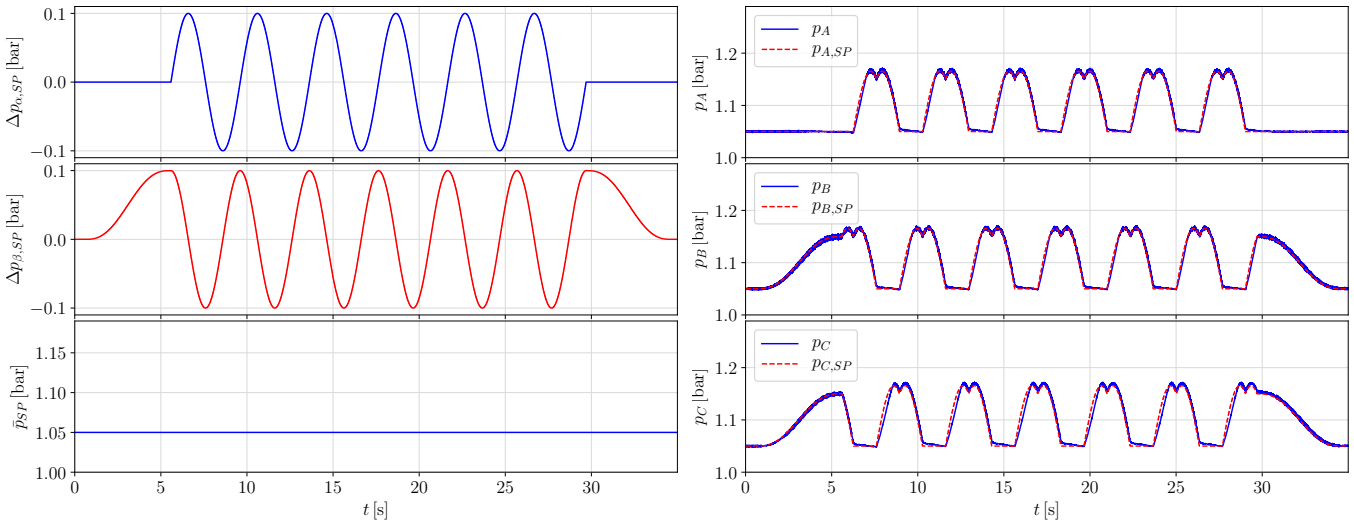

Fig. 3. The figure shows the relation between the pressure setpoint trajectories in the Delta Representation space (left) and the resulting trajectories in the absolute pressure space (right), for a simultaneous excitation in Δp_α and Δp_β. Notice that at least one pressure p_i, $i = A, B, C$ is restricted to $\bar{p}$ at all times. The invariance property with respect to the integral is satisfied between $t = 5.6\,\mathrm{s}$ and $t = 29.6\,\mathrm{s}$.

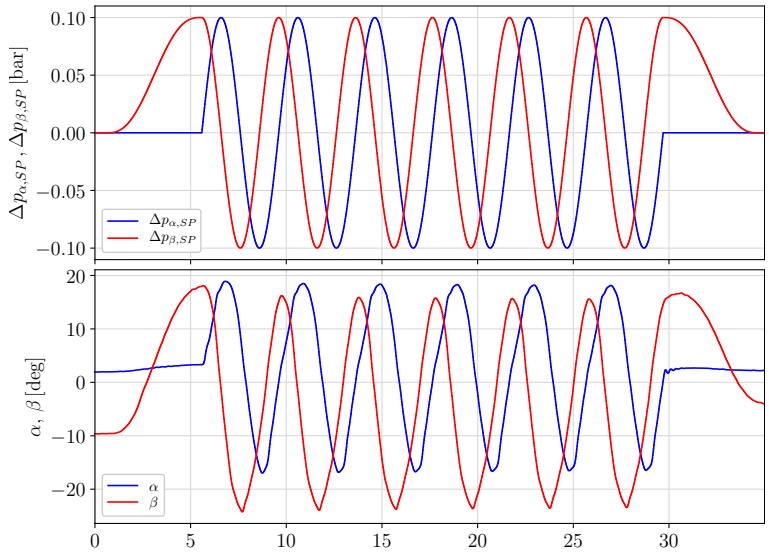

Fig. 4. The figure shows the result of a verification experiment of the decoupling characteristics of the Delta Representation, for a simultaneous excitation in Δp_α and Δp_β. The value of $\bar{p}$ is fixed at 1.05 bar.